Paper No. 212

Additional applications of active twist blades

Johannes Riemenschneider[*], Martin Pohl[*], Martin Schulz[*], Steffen Opitz[*], Thomas Hoffmann[*], and Frauke Hoffmann[†]

[*]Institute of Composite Structures and Adaptive Systems, Lilienthalplatz 7, 38108 Braunschweig, Germany

Johannes.Riemenschneider@dlr.de

[†]Institute of Flight Systems, Lilienthalplatz 7, 38108 Braunschweig, Germany

Frauke.Hoffmann@dlr.de

Abstract

Active Twist Rotor Blades have been developed for the use in secondary control such as higher harmonic control (HHC) and individual blade control (IBC). The basic principle of such blades is the implementation of piezoelectric actuators into the blades, using different types of coupling, causing the blades to twist. At the DLR model scale blades have been manufactured to demonstrate the feasibility of such systems. This paper is describing two other types of application of such blades.

De-icing a rotor blade using the pre-existing actuators. The working principle for de-icing the blade is to excite vibrations with high amplitudes. These vibrations break up and shake off the ice. The centrifugal forces clear the ice off the rotor blade; however, the stiffening effect caused by the rotation reduces the amplitude of the bending modes, which are the most influential factor in breaking up the ice. First tests have been made using a 50 cm long blade segment. A setup was established to grow different types of ice on the blade within a freezer between -10° C and -25° C in a non-rotating system. It could be shown that glaze ice could be broken easily. Next steps will be the test of the effectiveness to remove ice in a rotating system, where more realistic ice formations will be generated. Also it has to be examined how good the system works for rime ice.

Manipulation of damping using blade integrated actuators. The idea is to use blade integrated actuators as part of electromechanical absorbers. Using certain electrical networks, the structural behavior of the rotor blade can be significantly influenced. The effectiveness of such systems to increase the structural damping of an active twist blade was experimentally investigated. The operation of different sets of actuators allowed the excitation of individual modes. At first an oscillating circuit was established coupling the capacitive piezoelectric actuators with an inductivity. If the setup is tuned right, this results in a significant decrease of the amplitudes of a single frequency, e.g. torsional eigenfrequencies. In a next step a virtual "negative capacity" was used to dissipate the vibrating energy in the electrical circuit. Such an element shows the same amplitude response as the capacity, but the phase is shifted by 180 deg compared to a "regular capacity". The advantage of this method is the effectiveness over a broad frequency range. That way several modes can be influenced at the same time. Finally, a first evaluation of the influence of these measures on the vibration level of a complete rotor was carried out.

PRINCIPLES OF ACTIVE TWIST

The basic principle of individual blade control and its benefits for an improved aerodynamic behavior has been shown in many different studies [1]. The goals are vibration reduction, noise reduction and performance improvement. One concept which has been investigated in detail is active twist. For several years the German Aerospace Center (DLR) has been investigating this technology and built several model rotor blades. A history of these activities can be found in [2, 3, 4]. The basic principle of this technology are skin integrated patch type actuators to introduce shear strain into the skin. Piezoceramic d_{33} actuators can be used for such purposes. The commercially available Macro Fiber Composites (MFC, see figure 1) were used for the DLR blades. Also the dynamics needed to excite a blade at frequencies up to 100 Hz is given by these actuators. Due to the use of the d_{33}-Effect these actuators show strains of up to 1600μm/m.

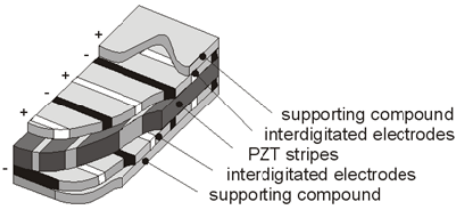

Figure 1: Piezoceramic actuator using the d_{33}-Effect: MFC by NASA.

With the given electrode spacing of the MFCs voltages up to 1500V are necessary to yield these active strains. The design of the skin can be optimized in order to maximize the twist angle, the twist momentum or the twist work (see also [5]). The relation between the momentum M, the twist rate θ' and the torsional rigidity GI is given by the following equation.

$$M = \theta' \cdot GI$$

One of the model rotor blades built by DLR is the AT4. The geometry is based on a mach scaled BO 105 model blade with a radius of 2 m. It is optimized for maximum momentum. The GFRP skin is assembled of unidirectional plies at an angle of $\pm 45°$. The actuation system of the AT4 is composed of 26 Macro Fiber Composite actuators that are integrated in the upper and lower skin of the blade (see Figure 2). The working direction of

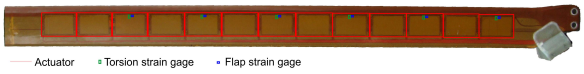

Figure 2: AT4

the actuators is in $\pm 45°$ with respect to blade axis. Hence strain is induced in the main stress direction of the torsion and forces the blade to twist. To have a maximum in control flexibility the blade itself is wired in a way that allows to operate several actuator segments separately (see figure 7).

In the following sections two other types of application for such blades are shown: de-icing of rotor blades and manipulation of structural damping.

DE-ICING

Icing of helicopter rotor blades is a serious problem. The most dangerous effect of ice on rotor blades is the possibility of losing the aerodynamic lift [6]. In contrast to fixed-wing aircrafts a de-icing system for helicopters is still not a standard. There are numerous de-icing systems for helicopters that have been studied [7]. However, industry offers just an electro-thermal de-icing system for a limited number of helicopter models. This is due to the harsh environment in which the rotor blades operate, for example high centrifugal and aerodynamic forces, connection between fixed and rotating part, temperatures between -30°C and 70°C as well as rain and sand erosion.

The thought behind this study is to use the already available actuators of the active twist blade as a potential de-icing system. The basic principle for de-icing the blade goes back to the 70s [8], where different shakers are introduced into metal blades to excite vibrations which successfully cause shear forces between the ice and the blade. These vibrations break up and shake off the ice. The centrifugal forces clear the ice off the rotor blade; however, the stiffening effect caused by the rotation reduces the amplitude of the bending modes, which are thought to be the most influential factor in breaking up the ice.

A segment of an active twist blade served as test platform for the first experimental investigations performed at DLR (see Figure 3). The specimen is a $0.5m$ segment of the airfoil section of a Mach-scaled Bo105 rotor blade (NACA 23012 airfoil) with a radius of 2 m and a chord of 121 mm. To grow the ice the segment is installed in a freezer with ambient temperatures between -10°C to -25°C. In this icing environment water is sprayed onto the blade, where it freezes. In the current set up the Mean Volume Droplet diameter (MVD) cannot be exactly adjusted. Different types of ice (rime ice and glaze ice) can be generated depending on the temperature and the water mass flow. A clear distinction between freezer ice and impact ice as described in [9] can not be made, since both types of ice accrete on the blade (see Figure 5). The blade stands still and water is sprayed on it. Hence the created ice shapes differ from typical ice shapes of rotating blades (see [10]). The ice formation realized within this test rig is more comparable to accretion of ice for the helicopter standing on the airfield.

Different excitations are investigated to shed the accreted ice. First of all an experimental modal analysis of the clamped blade segment is performed to find its eigenfrequencies. In a first set up one signal generator and amplifier excite all piezoelectric actuators. That means that all actuators

Figure 3: Blade segment with accreted ice at the leading edge

operate in phase. Exciting the blade with the first torsion eigenfrequency leads to the highest displacement and strain amplitudes. Due to deformation coupling the vibration mode is a mixture of the first torsion and third bending mode (see Figure 4). The ice can be cracked in large regions (1 and 2) when the actuators are switched on (see figure 4).

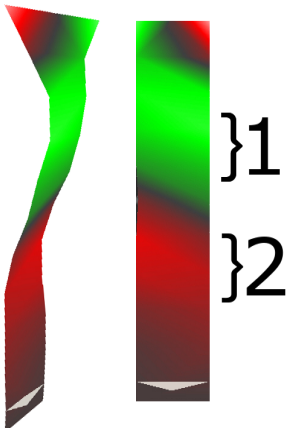

Figure 4: Forced oscillation mode at first torsion frequency

Ice at the nodes of this vibration does not shed in the same way. If the before described excitation lasts for several seconds (e.g. 30 sec) the remaining ice comes off, because the blade heats up and that decreases the ice adhesion strength. Another possibility to shake off the remaining ice is to excite eigenmodes, which have nodes at other locations. But the resulting amplitudes of these modes are significantly smaller than the amplitudes of the first torsion mode, because the design is not optimized to excite these modes. The deformation induced by this vibration is not large enough to overcome the ice adhesion strength immediately.

It is planned to do future investigations with individual excitation of each actuator to optimize the de-icing effect. A Finite Element Model is under preparation to get a better inside in the stress distribution on the blade surface and to estimate the influence of the centrifugal forces.

Figure 5: Rotor blade with accreted ice and spontaneous cracks in the ice due to torsion deformation

Obviously there are still many open questions, like the influence of this de-icing strategy on the aerodynamics of the helicopter, the vibration levels in the cabin and fatigue issues. As the deicing of rotation blades is the goal of this research, it is planned to perform icing and deicing in a rotary test stand.

DAMPING MANIPULATION

Theoretical Background

”Piezoelectric shunt damping” subsumes all concepts, where an oscillating structure is damped with applied piezoceramic actuators connected to electric shunt networks. The basic principle can be seen in Figure 6. As shunt network, different combinations of electronic components can be used. According to the use of active and passive components, shunt networks can be divided into groups, depending on their need for external energy supply. Systems that do not require external electric energy are called *passive*. If a small external power supply is needed, they are called *semi-active*. In contrast to active vibration control,

no separate sensors, controllers or actuator amplifiers are needed.

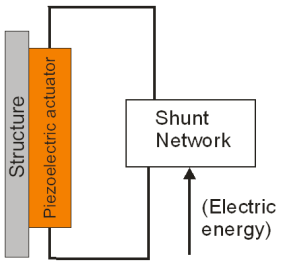

Figure 6: Principle of piezoelectric shunt damping

First Attempts of piezoelectric shunt damping were performed by Hagood and Flotow in 1991 [11] with the theoretical and experimental investigation of simple passive R and RL networks, comparable to better-known mechanical spring mass vibration absorbers. Hollkamp and Starchville 1994 introduced a self-adjusting RL network with a synthetic inductor [12], able to tune to changed system eigenfrequencies. Like a mechanical vibration absorber, RL networks can also only damp one eigenfrequency. Hollkamp [13], Wu [14] and Behrens et al. [15] introduced several possibilities of multiple-mode RL damping networks consisting of passive RL shunts combined with LC filters to access several eigenfrequencies. They were able to show the feasibility of damping more than one eigenfrequency with one single piezoelectric actuator by splitting the shunt network into branches for every single mode. By this, these concepts are usable for continuum oscillators with a lot of different vibration modes. The most important drawback of all passive shunt networks is, that it is not possible to tune them easily, and that inductivities typically needed for shunting can get very bulky when the inductance values exceed a few Henries.
For rotating structures like rotor blades, the eigenfrequencies are varying with rotation frequency. That is why such damping concepts cannot be used, because every shift in the eigenfrequencies would require a retuning of the shunt system. In 2003, Park [16] introduced the negative capacitance shunt, a semi-active network which also can be used to damp oscillating structures. The great advantage of this system is its broadband effect, which is nearly independent from the excitation frequency, but with the same efficiency as the passive RL shunts. This qualifies such shunt networks for the use in a mechanical system with a lot of varying eigenfrequencies.
Initial tests of the negative capacitance shunt network at the DLR revealed an excellent broadband damping effect of up to 20dB maximum in vibration amplitude over a frequency range of approx. 0-3kHz [17] on a rotating circular saw blade as test object.

Measurement method

In order to measure the effect of damping an active rotor-blade by using passive and semi-active shunt-networks a series of experimental investigations were performed. In these tests the active twist model rotor-blade "AT4" is used (see figure 2). As described earlier 26 piezio-electric actuators are applied on the surface. (13 at each surface, see figure 7). For damping the blade by shunt-networks, the inner 7 segments of the upper and lower surface were used in different networks. This is the region of maximum strain for the first torsion eigenfrequency.

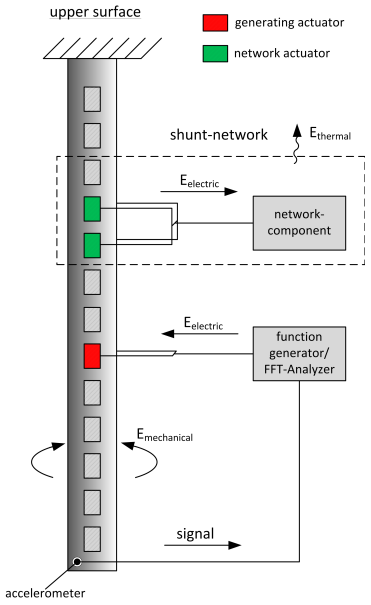

Figure 7: test preparation and energy-flow

The test set-up (figure 7) shows, that the AT4 rotor-blade is clamped at the blade root in vertical position. The eighth actuator is used for torsional excitation of the blade. A function generator excites the blade with a frequency sweep-signal up to 200 Hz, which includes the first and second torsional-eigenfrequency of the AT4. For measuring the vibration of the blade, an acceleration sensor is placed at its tip. To record the damping-impact

of different shunt-networks, a frequency-response-function (FRF) of the system is created by a FFT-analyser. To evaluate the results of the FRF the Matlab-based tool "X-Modal II" by the University of Cincinnati was used.

To modify the damping characteristics of the AT4-blade a RL-network for damping a single frequency and a negative capacitance-network for realizing a broadband-damping had been used.

RL-shunt-network

The RL-shunt-network as shown in figure 8 behaves like a tuned-mass-damper, so it is needed to tune inductance and capacitance to the eigen-frequency of the rotor that is to be damped. The capacitance is a fixed value given by the design of the piezo-actuator. That is why the inductance is used to set the eigenfrequency of the resonant circuit.

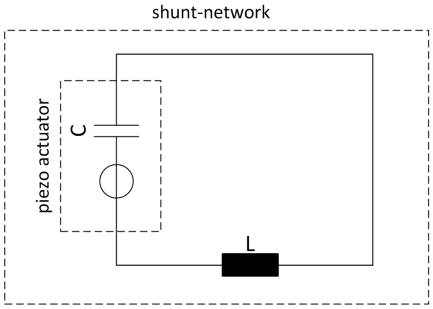

Figure 8: LC-circuit

Lower frequencies and small capacitance lead to large inductances. I.e. an actuator with a capacitance of $20nF$ that should be used to damp at a frequency of $50Hz$ needs an inductance of $\approx 507H$. A synthetic inductance, which simulates the behavior of an inductor by using a capacitance, is very useful for a compact realization [18]. In resonance, reactance of capacitance and inductance cancel each other out. Thereby a voltage overshoot emerges at inductance and capacitance, which causes higher current and the energy is dissipated into heat of the resistance [19].

Variable number of blade-actuators: Measurement-series with different numbers of actuators were recorded in order to show the increase of damping of the networks. Thereby the impact of the actuator position as well as the number of connected actuators is investigated. At positions with high blade-strains (in the damped eigenform), actuators deliver high voltage, which corresponds to high electrical energy to introduce into the network [17]. Damping will be maximized when actuators at these locations are used.

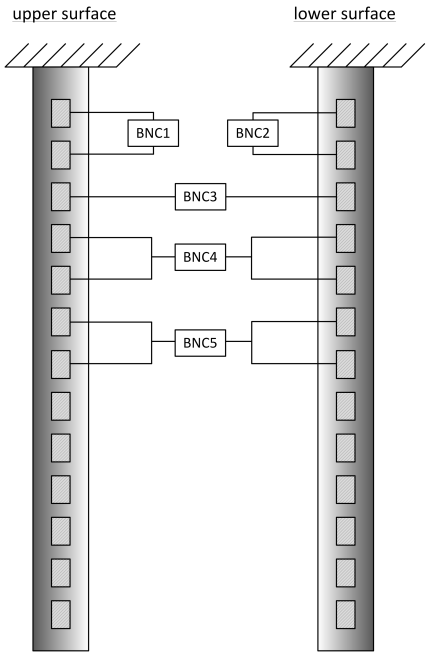

Figure 9: combined actuator segments

The wiring of the individual actuators of the balde is shown in figure 9. During the measurement different configurations were successively shunted.

Due to the different strain levels and different capacities of the actuators, the inclusion into one network will lead to currents between the actuators. Those currents decrease the damping-effect of the whole network.

In the first measurement the LC-circuit was tuned to a frequency of $55.0Hz$. This matches with the first torsional-eigenfrequency of the rotor blade. The measurements show a typical absorber-behavior for the application of different networks (figure 10).

An increasing number of actuators, which means a higher capacitance and electrical charge, increases the absorber-effect of the network. Secondary resonances (s.r.) are created. They are located between $52.75Hz$ and $58.0Hz$. The maximum achieved amplitude reduction reaches $\approx 13.2dB$ at the resonance frequency (equal to

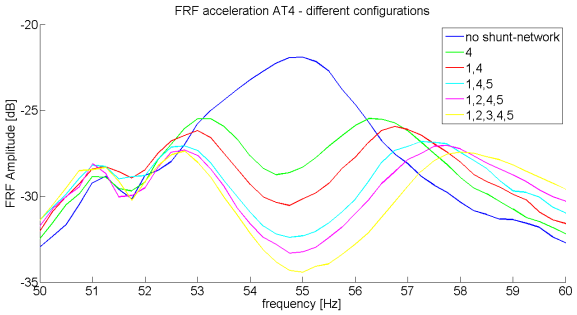

Figure 10: FRF of the damped AT4-blade with increasing network-number

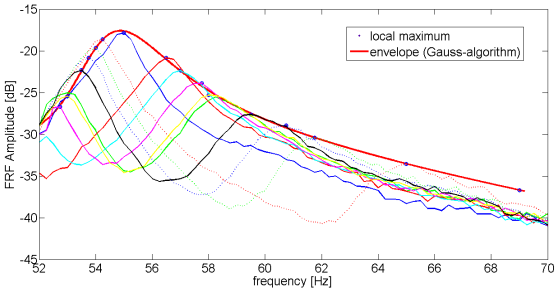

Figure 11: development of secondary resonances with envelope

LC-circuit-frequency). The amplitude at the secondary resonance-points could get reduced for about $5.5dB$ (for both) in relation to the amplitude with no shunt-network. More values are listed in table 1.

port (shunt-network)	LC-eigenfrequency $[Hz]$	reduction amplitude-ratio $[dB]$		
		LC_{reso}	$s.r.1$	$s.r.2$
4	55.00	7.55	3.32	3.46
1,4	54.50	9.25	4.26	3.90
1,4,5	54.75	11.10	4.87	4.94
1,2,4,5	55.00	12.24	5.03	5.07
1,2,3,4,5	55.00	13.21	5.39	5.55

Table 1: influence of different segment combinations

Shifting LC-circuit–frequency: In a rotating blade of a helicopter, high centrifugal forces influence the stiffness of the blade. An increasing stiffness leads to a shifting eigenfrequency as seen in the relation

$$\omega_0 = \sqrt{c/m}.$$

To investigate the influence of those changing frequencies to the damping of an RL-shunt-network, a measurement with shifting LC-frequencies was carried out. The results show that a variation of the LC-frequency for only about $-3Hz$ results in a decrease of maximum amplitude-ratio-reduction to $8dB$ (related to the first measurement without shunt-network).

At an increase of $10Hz$, a reduction of the amplitude-ratio referred to the non-shunt-network-measurement (at $55.0Hz$) of $2dB$ could still be reached (see figure 11). The dominating left secondary resonance-amplitude was reduced only about $0.74dB$ related to the measurement without shunt-network. More results are shown in table 2.

frequency $[Hz]$			reduction at	reduction at s.r. 1	reduction at s.r. 2
LC	s.r. 1	s.r. 2	eigenfreq. $[dB]$	$[dB]$	$[dB]$
54.25	52.75	57.75	14.88	8.86	6.04
55.00	53.00	58.00	16.76	7.59	7.44
56.25	53.50	59.50	13.25	4.45	9.78
57.75	53.75	60.75	10.25	2.98	11.08
58.75	54.00	61.75	8.02	1.80	12.56
62.00	54.25	65.00	4.67	0.79	15.70
65.75	54.25	69.00	2.95	0.74	18.86

Table 2: influence of different LC-frequencies

LC-circuit with additional resistance: As a result of the shifting-frequency-measurement, it can be concluded, that the damping of the blade has to be increased in a wider band of frequencies. To realize a small bandwidth of damping with the RL-network an additional resistance can be added (see figure 12).

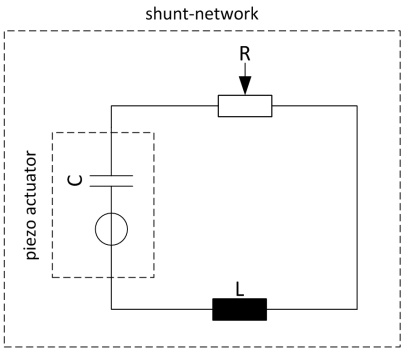

Figure 12: RLC-circuit with variable R

This causes a reduced amplitude-ratio of the secondary resonances, but a raise of the amplitude-ratio of the LC-frequency. So this type of damping with a RL-shunt-network is a compromise of an increase of damping at secondary resonances and a decrease at the torsional-eigenfrequency. The additional resistance behaves like a damper in a mechanical mass-spring-damper-system. To reduce the effect of secondary resonances, the resistance

can be increased stepwise. In table 3 the reduction of the amplitude-ratios between non-shunt-network-measurement (at $55.0Hz$) and additional-damped-measurements (at secondary resonance 1 and 2, amplitude at $55.0Hz$) of the FRF are shown.

The resistance is tuned in a way, that resulting characteristics do not show the individual secondary peaks and a minimum, but rather some kind of plateau. At this condition, the first torsion eigenfrequency could get reduced for about $8.3dB$. With an additional resistance of $\approx 1500\Omega$, secondary resonances vanished completely and a single resonance appeared. The curves of increasing resistance are shown in figure 13.

addiotional resistance $[\Omega]$	reduction at $55Hz$ $[dB]$	reduction at s.r.1 $[dB]$	reduction at s.r.2 $[dB]$
300	12.28	6.15	6.44
900	9.82	6.68	7.55
1500	8.32	6.53	8.22
1800	7.71	–	–
5000	4.90	–	–

Table 3: amplitude-reduction influenced by an additional resistance

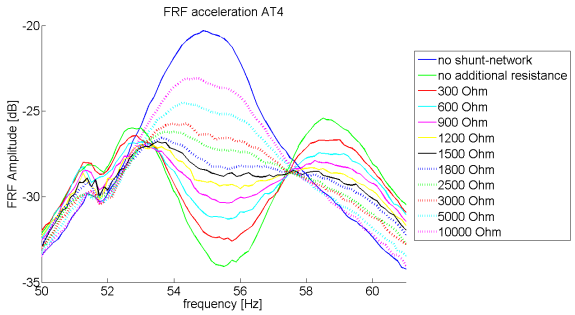

Figure 13: FRF of AT4 with variable additional resistance

Negative-capacitance-network

A better possibility for realizing a broadband damping is a negative capacitance network. In this type of shunt network, a negative impedance converter generates a phase-offset of 180° at a second capacitance (see Figure 14).

So the reactance compensates not just at one frequency like for the LR-circuits, but broadband and the electric energy transforms into heat at the system resistance. This principle illustrates that the capacitance-ratio between the piezo element and the negative impedance has to be (in best case)

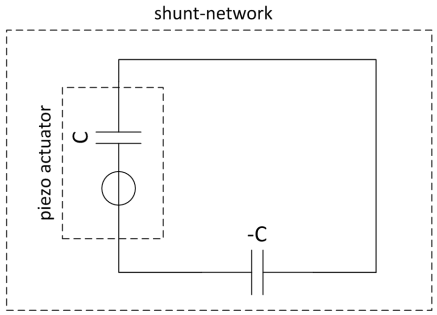

Figure 14: negative capacitance-network

1 in order to draw the highest amount of electrical energy out of the system. To show the influence of the capacitance-ratio on damping of the rotor blade, a characteristic curve of one shunt-network for one actuator-segment has been recorded (see figure 15). As seen, the highest damping was reached at a ratio of nearly 1, which corresponds to the literature [20].

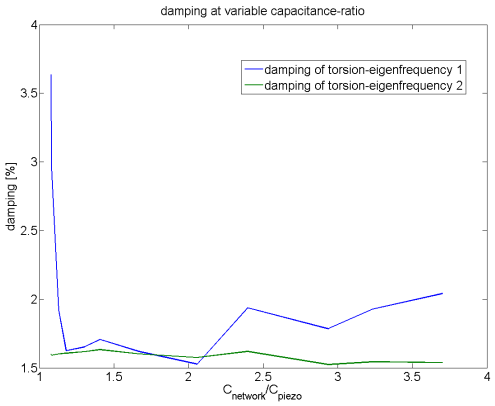

Figure 15: damping of the AT4-blade at variable capacitance-ratio

For a multimodal-damping an optimal actuator-position and/or higher number of actuators is required to achieve high damping-results. Thereby a bigger part of mechanical energy can get transformed into electrical energy. There are two alternatives to connect the actuators to the damping-network. First, every actuator segment can get one single network. Second, all actuators get shunted to one network in parallel. The effects of those variants to damping are shown in the following two sections.

Individual negative-capacitance-networks: In this measurement every single blade-actuator-port ($1-5$, see figure 9) was connected to an extra network. The results showed that the damping could be increased at the first as well as second torsion eigenfrequency (see figure 16).

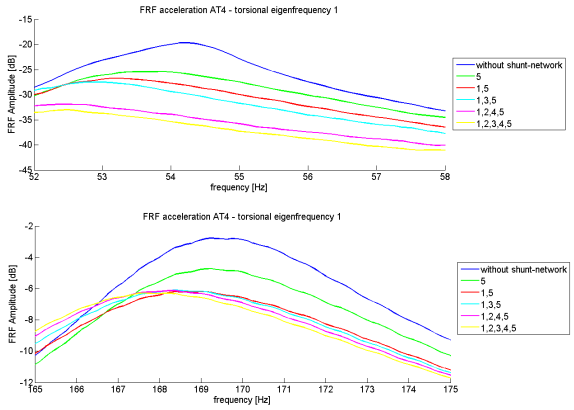

Figure 16: characteristics of increasing actuator-segments

Some values for different configurations are listed in table 4. At a capacitance-ratio near 1, an increase of damping from 1.8% up to 5.7% was measured for the first torsional eigenfrequency. In the second torsion-eigenfrequency the damping increased from 1.9% up to 2.7%. The increase of damping was attended by a decrease of the first eigenfrequency up to $3.4Hz$ and the second up to $1.5Hz$.

port	t-ef $[Hz]$		$C_{network}/C_{piezo}$	damping $[\%]$	
(shunt-network)	1	2		1	2
–	54.375	169.380	–	1.8173	1.9381
5	53.500	169.250	1.010	3.3283	1.9057
1,5	53.250	168.630	1.025	3.3369	2.4353
1,3,5	52.750	168.380	1.039	3.1854	2.4543
1,2,4,5	51.125	168.380	1.006	5.2018	2.5653
1,2,3,4,5	51.00	167.750	1.016	5.6627	2.6565

Table 4: damping with individual shunt-networks

Actuators connected to a single negative-capacitance-network: For this measurement all actuators were connected in parallel to one network. The number of connected actuators was varied. The results for damping of the first torsional eigenfrequency show no remarkable differences in its characteristics compared to the measurement with individual negative capacities connected to each actuator. But indeed the damping of the second torsional eigenfrequency did not increase (see table 5). This is due to the fact, that for the second eigenmode the actuators undergo very differing deformations (see figure 17), which results in compensation-currents between the actuators. Thus, shunted actuators to one network in the tested configuration were not suited for damping the second torsion-eigenmode.

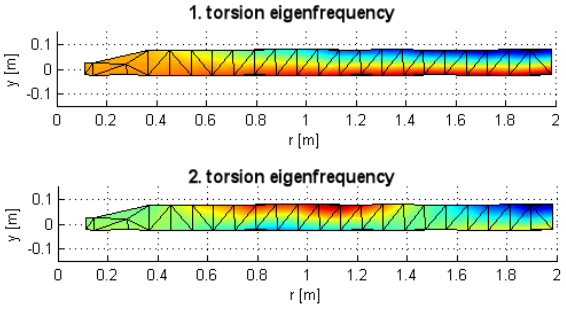

Figure 17: displacement of the AT4 in 1st and 2nd torsion eigenfrequency

port	t-ef $[Hz]$		$C_{network}/C_{piezo}$	damping $[\%]$	
(shunt-network)	1	2		mode 1	mode 2
-	54.250	170.000	-	1.7102	1.7192
5	53.500	169.50	1.026	3.4651	1.8477
1,5	53.125	169.250	1.034	3.5022	1.6911
1,3,5	51.375	169.250	1.026	4.7016	1.6307
1,2,4,5	53.125	169.250	1.190	6.882	1.7606
1,2,3,4,5	53.625	169.250	1.014	6.1854	1.5943

Table 5: damping with shunted actuators to a single network

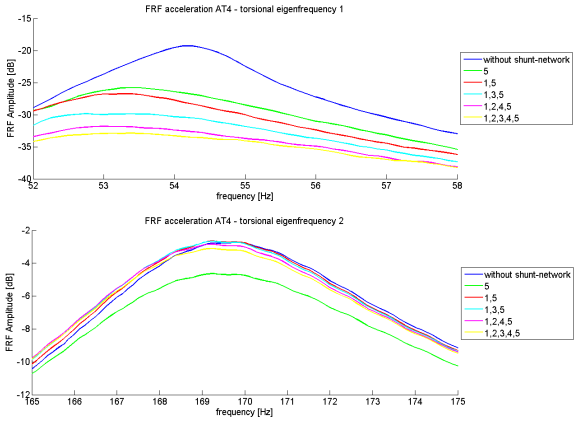

Figure 18: damping with shunted actuators to one network

Influence on the helicopter vibration suppression

In order to examine the influence of the described shunted negative-capacitance-networks and the

resulting structural damping changes of the rotor blades torsional response, some rotor simulations in forward flight were carried out. A Bo105 model rotor was analyzed exemplary via computations with the DLR rotor comprehensive aeromechanics code S4 [21, 22, 23, 24]. The Mach scaled model rotor has a radius of 2m and possesses the same blade dynamics as the full-scale Bo105 rotor. Since vibratory loads are of major importance in high speed forward flight, an advance ratio of μ=0.36 was chosen for the calculations. The shaft angle was set to $\alpha_{sh} = -13.3°$, and a rotor loading of C_T/σ = 0.07 was applied. The two different network configurations were compared to the baseline case without a capacitance-network. The baseline case was computed with a torsional damping value of 1.25% which can be taken as a typical damping value for conventional rotor blades. For a single shunted network a torsional damping of 6.2% for the first torsion mode and a damping of 1.6% for the second torsion mode was chosen (see table 5). The effect of the individual networks were examined with damping values of 5.7% and 2.7% for first and second torsion mode referring to table 4. All computations assume the change of structural damping with rotational speed to be negligible.

The degree of rotor vibration can be estimated from the 4/rev force and moment components of the hub loads in the non-rotating frame, since these components represent the main source for vibration excitation of the helicopter airframe.

The resulting force and moment magnitudes as computed for high speed forward flight are shown in figure 19 where a clear effect of the increased torsional damping on the vibrations compared to the baseline case can be found for all components. Slightly higher reductions are visible for the individual networks but both, individual and single network configuration, basically result in vibration reductions of approximately 30%, using just a few watts of electrical energy.

This amount of vibration reduction is not as significant as predicted for active methods, that need significantly more energy, as summarized in [25, 26]. Usually, actively controlled rotor blades aim to an advantageous change in the aerodynamic loads of the system with regard to noise and vibration reduction as well as minor performance enhancement. Here, mostly a re-distribution of the rotor lift is achieved through the higher harmonic control angle [27, 28]. From figure 20 it becomes visible that the effect of an increased torsional damping is

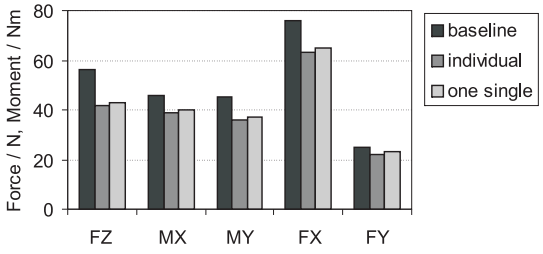

Figure 19: 4/rev force and moment components of the hub loads

only marginal with regard to the torsion response of the rotor blade (where ϑ is the tip pitch and ψ is the azimuth). Therefore, the change in the aerodynamic loads and accordingly the difference in rotor vibration can be expected to be rather small which is confirmed by the results illustrated in figure 19.

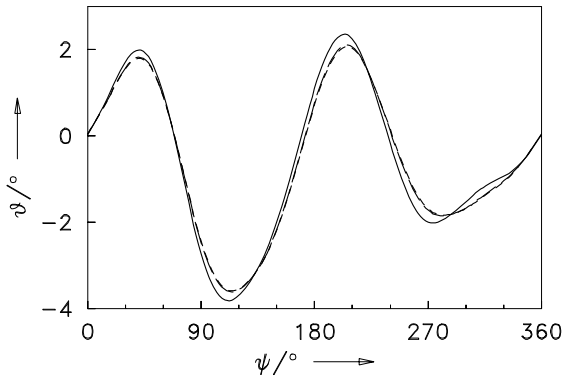

Figure 20: Elastic torsion response of the rotor blade for the baseline case (solid), one single (dashed) and individual (dotted) network

Although, a structural damping of the flap modes probably would be more effective with regard to the vertical vibratory loads, the aerodynamic damping can be assumed to be dominating towards the structural damping for flapping. Hence, an increased structural damping probably would not be effective with respect to flapping.

Conclusions

In this paper the possibility to do de-icing with active twist blades was presented. First experiments show, that specific actuation can cause ice to break and to detach from the blade surface. This

is a promising start and further investigations are still to come.

In the second part of this paper a technology of shunting was presented to influence the damping ratio of an active twist blade (equipped with piezoceramic actuators). Besides the use of an LC-circuit also the broad band method of negative capacities was presented. Different of these networks were designed, built and tested on a model rotor blade with active twist actuators. With this semi passive manipulation (low external energy) an increase of the structural damping up to 6% was achieved. First rotor dynamic calculation show, that this can result in a decrease of the vibratory loads for high speed forward flight of about 30%. Since there are no current costs for this technology such as energy input, additional weight, this is a great addition to any piezo actuator based active twist blade to be considered while the active control is not used.

REFERENCES

[1] Christoph K. Maucher, Boris A. Grohmann, and Peter Jnker. Review of adaptive helicopter rotor blade actuation concepts. In *Adaptronic Congress*. Adaptronic Congress, 2006.

[2] Hans P. Monner, Steffen Opitz, Johannes Riemenschneider, and Peter Wierach. Evolution of active twist rotor designs at dlr. In *AIAA/ASME/AHS Adaptive Structures Conference, Schaumburg, IL, USA*, 2008.

[3] Hans P. Monner, Johannes Riemenschneider, Steffen Opitz, and Martin Schulz. Development of active twist rotors at the german aerospace center (dlr). In *AIAA/ASME/AHS Adaptive Structures Conference, Denver, CO, USA*, 2011.

[4] Peter Wierach, Johannes Riemenschneider, Steffen Opitz, and Frauke Hoffmann. Experimental investigation of an active twist model rotor blade under centrifugal loads. In *33rd EUROPEAN ROTORCRAFT FORUM*, Kazan, Russia, 2007.

[5] J. Riemenschneider, P. Wierach, and S. Keye. Preliminary study on structural properties of active twist blades. Friedrichshafen, ERF 2003, Sep 2003. Friedrichshafen, ERF 2003, 29th European Rotorcraft Forum.

[6] R. W. Gent, N. P. Dart, and J. T. Candsdale. Aircraft icing. *Philosophical Transactions of Royal Society of London Series A*, 358:2873–2911, 2000.

[7] H. J. Coffman. Helicopter rotor icing protection methods. *Journal of the American Helicopter Society*, 32(2):34–39, 1987.

[8] H.E. Lemont, H. Upton, Army Research, and Technology Laboratories (U.S.). Applied Technology Laboratory. *Vibratory ice protection for helicopter rotor blades*. USAAMRDL-TR. The Laboratory, 1978.

[9] E. W. Brouwers, J. L. Palacios, A. A. Peterson, and E. C. Smith. The experimental investigation of a rotor hover icing model with shedding. Phoenix Az., 2010. American Helicopter Society Conference.

[10] E. W. Brouwers, A. A. Peterson, J. L. Palacios, and L. R. Centolanza. Ice adhesion strength measurements for rotor blade leading edge materials. Virginia Beach, VA, 2011. American Helicopter Society Conference.

[11] N.W. Hagood and A. von Flotow. Damping of structural vibrations with piezoelectric materials and passive electrical networks. *Journal of Sound and Vibration*, 146(2):243–268, 1991.

[12] J.J. Hollkamp and T.F. Starchville. A self-tuning piezoelectric vibration absorber. *Journal of intelligent material systems and structures*, 5(4):559, 1994.

[13] J.J. Hollkamp. Multimodal passive vibration suppression with piezoelectric materials and resonant shunts. *Journal of Intelligent Material Systems and Structures*, 5(1):49, 1994.

[14] S.Y. Wu. Method for multiple mode piezoelectric shunting with single pzt transducer for vibration control. *Journal of intelligent material systems and structures*, 9(12):991, 1998.

[15] E. Reithmeier, S. Mirzaei, and N. Kasyanenko. Optical vibration and deviation measurement of rotating machine parts. *Optoelectronics Letters*, 4(1), 2008.

[16] C.H. Park and H.C. Park. Multiple-mode structural vibration control using negative capacitive shunt damping. *Journal of Mechanical Science and Technology*, 17(11):1650–1658, 2003.

[17] M. Pohl and M. Rose. Vibration and noise reduction of a circular saw blade with applied piezoceramic patches and semi-active shunt networks. *proc. Adaptronic Congress Berlin*, pages 85–91, 2009.

[18] S.K. Mitra and C.F. Kurth. *Miniaturized and integrated filters*. Wiley, 1989.

[19] W. Weißgerber. *Elektrotechnik f ”ur Ingenieure: Wechselstromtechnik, Ortskurven, Transformator, Mehrphasensysteme*, volume 2. Vieweg+ Teubner, 2007.

[20] M. Neubauer, R. Oleskiewicz, K. Popp, and T. Krzyzynski. Optimization of damping and absorbing performance of shunted piezo elements utilizing negative capacitance. *Journal of sound and vibration*, 298(1-2):84–107, 2006.

[21] B. G. van der Wall. An analytical model of unsteady profile aerodynamics and its application to a rotor simulation programme. In *26th European Rotorcraft Forum*, Amsterdam, The Netherlands, 2000.

[22] T. S. Beddoes. A wake model for high resolution airloads. In *International Conference on Rotorcraft Basic Research*, Research Triangle Park, NC, USA, 1985.

[23] B. G. van der Wall. Simulation of hhc on helicopter rotor bvi emissions using a prescribed wake method. In *26th European Rotorcraft Forum*, Den Haag, The Netherlands, 2000.

[24] Y. H. Yu K. Pengel P. Beaumier B. G. van der Wall, C. L. Burley. The hart ii test, measurement of helicopter rotor wakes. In *Aerospace Science and Technology*, volume 8, 2004.

[25] C. Kessler. Active rotor control for helicopters: Individual blade control and swashplateless rotor designs. In *36th European Rotorcraft Forum*, Paris, France, 2010.

[26] C. Kessler. Active rotor control for helicopters: Individual blade control for helicopters: Motivation and survey on higher harmonic control. In *36th European Rotorcraft Forum*, Paris, France, 2010.

[27] R. Celi R. P. Cheng, C. R. Theodore. Effects of two/rev higher harmonic control on rotor performance. In *Journal of the American Helicopter Society*, volume 48, 2003.

[28] B. G. v. d. Wall. The effect of hhc on the vortex convection in the wake of a helicopter rotor. In *Aerospace Science and Technology*, volume 4, 2000.